Journal of the Franklin Institute 360 (2023) 14645–14659

Contents lists available at ScienceDirect

Journal of the Franklin Institute

journal homepage: www.elsevier.com/locate/fi

Event-triggered affine formation maneuver control for second-order multi-agent systems with sampled data

Suhui Ma [a], Dong Zhang [a,*], Yu Zhao [b], Chengxin Xian [b], Yuanshi Zheng [c]

[a] *School of Astronautics, Northwestern Polytechnical University, Xi'an 710072, PR China*
[b] *School of Automation, Northwestern Polytechnical University, Xi'an 710129, PR China*
[c] *School of Mechano-Electronic Engineering, Xidian University, Xi'an 710071, PR China*

ARTICLE INFO

Keywords:
Affine formation maneuver
Event-triggered control
Multi-agent systems
Second-order dynamic
Sampled data
Directed network

ABSTRACT

This paper addresses the affine formation maneuver problem for second-order multi-agent systems with distributed event-triggered controllers. For multiple leaders moving with constant accelerations, a sampled-data-based event-triggered proportional–integral controller is proposed to reduce the frequencies of controller update, where triggering moments are determined by the relative states between agent and its neighbors. Moreover, based on the proposed event-triggered control scheme, a self-triggered mechanism is designed to avoid continuous measurements for relative states and continuous calculating of local events at each discrete moment. Some sufficient conditions for achieving affine formation maneuver control are obtained and the Zeno behavior is naturally eliminated due to periodic sampling setting. Finally, the theoretical results are illustrated through numerical simulations.

1. Introduction

In recent years, formation control of multi-agent systems has attracted a lot of attention due to its wide applications in civil and military fields, such as commercial light show, resource exploration and target enclosing. This problem can be classified as static and dynamic formation control according to target formation shape. Static formation control focuses on generation and maintenance of a time-invariant geometric shape. Different from static formation control, dynamic formation control means that formation shape of all agents can change continuously, which has a more flexible respond to complex tasks and uncertain environments in cooperative systems, such as formation penetration and obstacle avoidance task in battlefield environments.

For dynamic formation control, there are two formation architectures in the existing research of multi-agent systems. The first one allows agents to form time-varying geometric configuration by using desired reference signals, e.g., time-varying absolute positions [1–4], time-varying relative displacements [5], constant displacements with time-varying weighting matrix [6,7], time-varying relative distances [8,9], and observer-based time-varying shape parameters [10]. However, in this architecture, expected dynamic signals always need to be designed offline in advance or online in real-time for each agent, which requires good storage or planning capability for all agents. Consequently, the formation control based on desired reference information is not suitable for dealing with emergent situations and large-scale systems. To overcome the disadvantages of using dynamic expected signals, the second architecture depends on special Laplacian matrix [11–19], whose constant weights involve desired nominal configuration information, and the corresponding mathematical transformation' invariance to parameters of formation geometric shape, such as collinearity and ratios of distance. Different from the first architecture, the second formation architecture has the advantage

* Corresponding author.
E-mail addresses: mmasuhui@163.com (S. Ma), zhangdong@nwpu.edu.cn (D. Zhang), yuzhao5977@gmail.com (Y. Zhao), xcx@mail.nwpu.edu.cn (C. Xian), zhengyuanshi2005@163.com (Y. Zheng).

https://doi.org/10.1016/j.jfranklin.2023.11.014
Received 6 February 2023; Received in revised form 11 May 2023; Accepted 5 November 2023
Available online 10 November 2023

that maneuverable configuration of agents can converge into the image space of nominal configuration without requiring global reference information. The typical dynamic formation control based on special Laplacian includes similar formation maneuver control [11–15], bearing-based formation maneuver control [16] and affine formation maneuver control [17–19]. Both similar and bearing-based formation maneuver control can ensure agents to continuously track target formations with time-varying translation, rotation and scaling transformations. And the difference between these two types of formation control is that the former is applicable to two-dimensional space and the latter is made available for arbitrary dimensional space. Compared with similar and bearing-based formation maneuver control, affine formation maneuver control can additionally realize shearing transformation based on nominal configuration in arbitrary dimensional space. Due to more abundant types of formation transformation in any dimensional space, affine formation maneuver control is more general and practical. Therefore, in this work, we adopt affine formation maneuver control to realize dynamic reconfiguration of formation.

Unlike the classic topology settings, e.g., undirected connected graph and directed spanning tree, affine formation control requires agents to equip with universally rigid or $d+1$-rooted networks for undirected or directed typologies in d-dimensional space, respectively. The special topologies tend to have more complex structures and more network links, which means a higher communication load. Therefore, the limitation of communication resources for affine formation maneuver control is an urgent problem to be solved.

Event-triggered control is an effective technology to save consumption of communication and computation resources in multi-agent systems, whose nature is to make agents only carry out necessary network transmission and control update. Although discrete triggering actions are driven by event-triggered control, the real-time states of agents are continuously monitored. In order to reduce resource usage caused by continuous detection, self-triggered control is developed, in which next triggering instants are predicted according to the last triggering information. Up to now, these two triggering control laws are mostly utilized for the formation based on time invariant/variant expected reference information [20–26] and static formation with special Laplacian [27–31], and are rarely applied to dynamic formation with special Laplacian [32]. The literature [32] proposes a distributed event-triggered affine maneuver formation control for first-order multi-agent systems, where parallel detection of position and velocity events is implemented. Unfortunately, composed of a proportional–differential triggering control law and the triggering mechanism with constant thresholds, this control strategy is nonperforming and demanding since it only guarantees the bounded convergence of tracking errors for followers and requires an acyclic network topology to avoid Zeno behavior. Thus, it is essential to develop efficient event-triggered or self-triggered control strategies for affine maneuver formation control problem, which can make a good balance between control performance and triggering efficiency.

Inspired by the above mentioned, we focus on affine formation maneuver control problem manipulated by sampled-data event-triggered and self-triggered mechanisms for second-order multi-agent systems containing multiple constant acceleration moving leaders in a direct communication network. The main contributions of this paper include:

(1) A distributed sampled-data-based event-triggered mechanism is designed to extent the proportional-integral affine formation maneuver control law reported in [17]. Compared with the existing event-triggered affine maneuver formation algorithm in [32], the proposed event-triggered control algorithm in this paper can ensure that the position states of all agents exponentially converge to the time-varying target configuration remaining the topology settings in [17].
(2) A self-triggered affine formation maneuver algorithm is presented, which can avoid continuous measurements of relative states and continuous calculating of local events at each sampling time compared with event-triggered ones proposed in this work and [32].
(3) Since sampled-data information is used in this paper, the proposed triggering algorithms does not exhibit Zeno behavior and is more practical for applications.

The remainder of this paper is organized as follows: Section 2 introduces necessary preliminaries and states problem. Distributed event-triggered and self-triggered affine formation maneuver algorithms are studied in Sections 3 and 4, respectively. Simulations are given in Section 5. Section 6 summarizes the results of this paper and indicates further research directions.

Notations. Let $\mathbb{R}$, $\mathbb{N}$ and $\mathbb{N}_{>1}$ denote the sets of real number, integer number and the integer number greater than 1, respectively. $\mathbb{R}^n$ and $\mathbb{R}^{n\times m}$ are the Euclidean spaces with dimensions $n\times 1$ and $n\times m$, respectively. $\mathbf{1}_n$ denotes the n-dimensional column vector with all entries equal to 1. I_n and $\mathbf{0}_{n\times m}$ denote the $n\times n$-dimensional identity matrix and the $n\times m$-dimensional zero matrix, respectively. $\|\cdot\|$ means the Euclidean norm. $\mathrm{Re}(\cdot)$ and $\mathrm{Im}(\cdot)$ means the real and image parts of a complex real number, respectively. A^T indicates the transpose of the matrix A. $diag\{a_1,a_2,\dots,a_n\}$ indicates the diagonal matrix with diagonal elements a_1 to a_n. $A\otimes B$ indicates the Kronecker product of matrices A and B. $\prod_{i=1}^n a_i$ represents the cumulative product from a_1 to a_n.

2. Preliminaries and problem statement

2.1. Preliminaries

The network topology of a group consisting of n agents is described by a signed weighted directed graph $\mathcal{G}=(\mathcal{V},\mathcal{E},\mathcal{W})$, where $\mathcal{V}=\{1,2,\dots,n\}$ is the vertex set, $\mathcal{E}\subseteq\mathcal{V}\times\mathcal{V}$ is the edge set, and $\mathcal{W}=[w_{ij}]_{n\times n}\in\mathbb{R}^{n\times n}$ is the signed weighted adjacency matrix. The edge $(j,i)\in\mathcal{E}$ represents that agent i can receive information from agent j, and agent j is an in-neighbor of agent i. The in-neighbor set of agent i is denoted as $\mathcal{N}_i=\{j\in\mathcal{V}:(j,i)\in\mathcal{E}\}$. In directed graph $\mathcal{G}$, $w_{ij}\neq 0\Leftrightarrow(j,i)\in\mathcal{E}$ and $w_{ij}=0\Leftrightarrow(j,i)\notin\mathcal{E}$. The elements of Laplacian matrix $L=[l_{ij}]_{n\times n}\in\mathbb{R}^{n\times n}$ of signed graph $\mathcal{G}$ are defined as $l_{ij}=-w_{ij}$ for any $i\neq j$ and $l_{ii}=\sum_{j=1}^n w_{ij}$ for any i. A path is an ordered combination of edges $\{(i_0, i_1), (i_1, i_2), \dots, (i_{l-1}, i_l)\}$, where $i_0, \dots, i_l$ are mutually different vertices. For directed graph $\mathcal{G}$, a vertex v is said to be k-reachable from a non-singleton set $\mathcal{U}$ if there exists a directed path form a vertex in the set $\mathcal{U}$ to vertex v after deleting any $k-1$ vertices except vertex v, which also means that there are k disconnected directed paths from set $\mathcal{U}$ to vertex v. The directed graph $\mathcal{G}$ is said to be k-rooted if there is a subset of k vertices called the root set, from which each other vertex is k-reachable. A spanning k-tree rooted at $\mathcal{R} = \{r_1, r_2, \dots, r_k\} \subset \mathcal{V}$ is a spanning subgraph $\mathcal{T} = (\mathcal{V}, \bar{\mathcal{E}})$ satisfying

(1) each vertex $r \in \mathcal{R}$ has no in-neighbor;
(2) each vertex $v \notin \mathcal{R}$ has k in-neighbors;
(3) each vertex $v \notin \mathcal{R}$ is k-reachable.

In this paper, we consider that there are m followers marked as agents 1 to m and $n-m$ leaders marked as agents $m+1$ to n in d-dimensional space. The sets of followers and leaders are denoted by $\mathcal{V}_f$ and $\mathcal{V}_l$, respectively. And $d \in \mathbb{N}_{>1}$. Suppose all leaders has no in-neighbors. Then, the Laplacian matrix L corresponding to the network topology $\mathcal{G}$ of multi-agent systems has the following form:

$$L = \begin{bmatrix} L_{ff} & L_{fl} \\ \mathbf{0}_{(n-m)\times m} & \mathbf{0}_{(n-m)\times(n-m)} \end{bmatrix}$$

where $L_{ff} \in \mathbb{R}^{m\times m}$ and $L_{fl} \in \mathbb{R}^{m\times(n-m)}$.

2.2. Problem statement

The double-integrator dynamic of follower $i \in \mathcal{V}_f$ is described by

$$\begin{cases} \dot{p}_i(t) = v_i(t) \\ \dot{v}_i(t) = u_i(t) \end{cases} \tag{1}$$

where $p_i(t) \in \mathbb{R}^d$ is the position, $v_i(t) \in \mathbb{R}^d$ is the speed and $u_i(t) \in \mathbb{R}^d$ is the control input. The dynamic of leader $i \in \mathcal{V}_l$ is described as follows

$$\begin{cases} \dot{p}_i(t) = v_i(t) \\ \dot{v}_i(t) = a_i \end{cases} \tag{2}$$

where $a_i \in \mathbb{R}^d$ is the constant acceleration.

A formation $\mathcal{F}_p$ of multi-agent systems (1)–(2) is composed of position $p = [p_1^T, p_2^T, \dots, p_n]^T = [p_f^T, p_l^T]^T \in \mathbb{R}^{nd}$ and directed network topology $\mathcal{G}$. The nominal formation of agents is described by $\mathcal{F}_q = (\mathcal{G}, q)$, where $q = [q_f^T, q_l^T]^T \in \mathbb{R}^{nd}$ indicates the nominal configuration. The affine span of configuration p is defined as $\mathcal{S}(p) = \{\sum_{i=1}^n a_i p_i \,:\, a_i \in \mathbb{R}, \sum_{i=1}^n a_i = 1\}$. The affine image of nominal configuration q is denoted as

$$\mathcal{A}(q) := \{p = (I_n \otimes A)q + \mathbf{1}_n \otimes b | A \in \mathbb{R}^{d\times d}, b \in \mathbb{R}^d\} \tag{3}$$

where (A, b) is the affine transformation. Rotation, scaling and shearing transformations to formation are described by matrix A, and translation transformation is denoted by vector b.

Definition 1. The affine formation maneuver is said to be achieved if the time-varying configuration $p(t)$ satisfies

$$\lim_{t\to\infty} p(t) = p^*(t) = (I_n \otimes A(t))q + \mathbf{1}_n \otimes b(t) \tag{4}$$

where $A(t)$ and $b(t)$ are continuous of t.

Assumption 1. The nominal configuration q_l of $n-m$ leaders satisfies $\{q_i\}_{i\in\mathcal{V}_l}$ affinely span in $\mathbb{R}^d$.

Assumption 2. The network topology $\mathcal{G}$ is $d+1$-rooted and the leader set is the root set.

Lemma 1 ([18]). *Under Assumption 1–2, the nominal formation $\mathcal{F}_q$ is affinely localizable in $\mathbb{R}^d$, that is,*

(1) For any $p \in \mathcal{A}(q)$ in $\mathbb{R}^d$, p_f can be uniquely determined by p_l;
(2) For formation $\mathcal{F}_p$, there exists a signed Laplacian matrix L corresponding to $\mathcal{G}$ satisfying $(L \otimes I_d)p = \mathbf{0}_{nd\times 1}$.

From Definition 1, it is clear that the target configuration $p^*(t) \subseteq \mathcal{A}(q)$ for all t. Assumption 1 implies that the column rank of matrix $[q_{m+1}, \dots, q_n; \mathbf{1}_{n-m}^T]$ is $d+1$ at least. According to [33, Lemma 2.1], Assumption 2 is equivalent to that $\mathcal{G}$ has a spanning k-tree rooted at leader set. Therefore, the nominal configuration and the network of multi-agent systems (1)–(2) are further designed by Assumption 1–2, respectively. Under the conditions of Lemma 1, the Laplacian matrix block L_{ff} is nonsingular and $\sum_{j=1}^n w_{ij}(p_j - p_i) = \mathbf{0}_{d\times 1}$ holds for any i. To achieve the affine formation maneuver, a real diagonal matrix $D = diag\{d_1, d_2, \dots, d_n\}$ needs to be configured such that matrix $\bar{L} = DL$ has $d+1$ zero eigenvalues and the rest with positive real parts, which implies that the nonsingular matrix block $-\bar{L}_{ff} = -diag\{d_1, d_2, \dots, d_m\}L_{ff}$ is Hurwitz. In this paper, we suppose the design of diagonal matrix D has been finished referring to the literature [18,33].

In fact, the expected trajectories $p_l^*(t)$ of leaders are described by the second-order polynomials from Eq. (2). And according to Lemma 1, the target time-varying configuration $p_f^*(t)$ of followers is $-(\bar{L}_{ff}^{-1}\bar{L}_{fl} \otimes I_d)p_l^*(t)$. Then the affine formation maneuver problem is equivalent to how to make $\sum_{j=1}^n w_{ij}(p_j(t) - p_i(t)) \to \mathbf{0}_{d\times 1}$ hold for any i while $t \to \infty$.

The main purpose of this paper is to design a triggering strategy such that the affine formation maneuver is still achieved for multi-agent systems (1)–(2).

3. Event-triggered affine formation maneuver algorithm

This section studies a distributed sampled-data-based event-triggered affine formation maneuver algorithm for multi-agent system (1)–(2), which is based on the proportional-integral control law proposed in [17].

3.1. Event-triggered affine formation maneuver strategy

In this paper, suppose that each follower is only allowed to measure relative state, transmit triggering information and update control input at each sampling instant lh, where $l \in \mathbb{N}$ and $h > 0$ is the sampling period. Let $t_k^i h$ denote the kth triggering instant for follower i. It is clear that $t_k^i h \subseteq lh$. Without loss of generality, assume $t_0^i = 0$ for any $i \in \mathcal{V}_f$.

Based on sampled-data, an event-triggered affine formation maneuver control law is designed as

$$\begin{cases} u_i(t) = -\alpha\iota_1 x_{pi}(t_k^i h) - \alpha\iota_2 x_{vi}(t_k^i h) - \beta\xi_i(t_k^i h) \\ \dot{\xi}_i(t) = \iota_1 x_{pi}(t_k^i h) + \iota_2 x_{vi}(t_k^i h) \end{cases} \tag{5}$$

where $t \in [t_k^i h, t_{k+1}^i h)$, $x_{pi}(t_k^i h) = d_i \sum_{j=1}^n w_{ij}(p_i(t_k^i h) - p_j(t_k^i h))$ and $x_{vi}(t_k^i h) = d_i \sum_{j=1}^n w_{ij}(v_i(t_k^i h) - v_j(t_k^i h))$ are the combinational measurement states of positions and velocities for follower i, respectively, $\xi_i(t)$ is the auxiliary variable, and control gains $\iota_1, \iota_2, \alpha, \beta > 0$. The event-triggered instant $t_{k+1}^i h$ for follower i is determined by

$$t_{k+1}^i h = \inf\{l : lh > t_k^i h, f_i(lh) \geq 0\} \tag{6}$$

where the event-triggered function $f_i(lh)$ is given by

$$f_i(lh) = \rho_1\|e_{pi}(lh)\| + \rho_2\|e_{vi}(lh)\| + \rho_3\|e_{\xi i}(lh)\| - \sigma_i(\rho_1\|x_{pi}(t_k^i h)\| + \rho_2\|x_{vi}(t_k^i h)\|) - \phi_i e^{-\gamma_i lh} \tag{7}$$

with some constants $\rho_1, \rho_2, \rho_3, \sigma_i, \phi_i, \gamma_i > 0$. In Eq. (7), $e_{pi}(lh) = x_{pi}(lh) - x_{pi}(t_k^i h)$, $e_{vi}(lh) = x_{vi}(lh) - x_{vi}(t_k^i h)$ and $e_{\xi i}(lh) = \xi_i(lh) - \xi_i(t_k^i h)$ denote the measurement errors.

Remark 1. Different from general proportional event-triggered control law, the measurement error $e_{\xi i}(lh)$ in Eq. (7) is specially set for the controller (5). States $\xi_i(lh)$ and $e_{\xi i}(lh)$ are obtained by using all triggering information $x_{pi}(t_k^i h)$ and $x_{vi}(t_k^i h)$ for each agent during the whole process of movement.

3.2. Stability analysis

Let $x_p(t) = [x_{p1}^T(t), \dots, x_{pm}^T(t)]^T$, $x_v(t) = [x_{v1}^T(t), \dots, x_{vm}^T(t)]^T$, $\xi(t) = [\xi_1^T(t), \dots, \xi_m^T(t)]^T$, $e_p(t) = [e_{p1}^T(t), \dots, e_{pm}^T(t)]^T$, $e_v(t) = [e_{v1}^T(t), \dots, e_{vm}^T(t)]^T$ and $e_\xi(t) = [e_{\xi 1}^T(t), \dots, e_{\xi m}^T(t)]^T$. Take the transformation $x_c(t) = -\beta(\bar{L}_{ff} \otimes I_d)\xi(t) + (\bar{L}_{fl} \otimes I_d)a_l$. Then denote $e_c(t) = -\beta(\bar{L}_{ff} \otimes I_d)e_\xi(t)$, $x(t) = [x_p^T(t), x_v^T(t), x_c^T(t)]^T$ and $e(t) = [e_p^T(t), e_v^T(t), e_c^T(t)]^T$. Hence, substituting Eq. (5) into Eqs. (1)–(2) yields

$$\dot{x}(t) = (A_1 \otimes I_d)x(t) - (A_2 \otimes I_d)x(lh) + (A_2 \otimes I_d)e(lh) \tag{8}$$

where

$$A_1 = \begin{bmatrix} \mathbf{0}_{m\times m} & I_m & \mathbf{0}_{m\times m} \\ \mathbf{0}_{m\times m} & \mathbf{0}_{m\times m} & \mathbf{0}_{m\times m} \\ \mathbf{0}_{m\times m} & \mathbf{0}_{m\times m} & \mathbf{0}_{m\times m} \end{bmatrix}, \quad A_2 = \begin{bmatrix} \mathbf{0}_{m\times m} & \mathbf{0}_{m\times m} & \mathbf{0}_{m\times m} \\ \alpha\iota_1\bar{L}_{ff} & \alpha\iota_2\bar{L}_{ff} & -I_m \\ \beta\iota_1\bar{L}_{ff} & \beta\iota_2\bar{L}_{ff} & \mathbf{0}_{m\times m} \end{bmatrix}$$

Lemma 2 (*[34]*). *For a third-order complex coefficient polynomial $f(s) = s^3 + c_1 s^2 + c_2 s + c_3$ ($c_i = c_{Ri} + \sqrt{-1}c_{Ii}$, $i = 1, 2, 3$), $f(s)$ has all its zeros in the left half-plane if and only if*

$$\Delta_1 = c_{R1} > 0, \quad \Delta_2 = \begin{vmatrix} c_{R1} & c_{R3} & -c_{I2} \\ 1 & c_{R2} & -c_{I1} \\ 0 & c_{I2} & c_{R1} \end{vmatrix} > 0, \quad \Delta_3 = \begin{vmatrix} c_{R1} & c_{R3} & 0 & -c_{I2} & 0 \\ 1 & c_{R2} & 0 & -c_{I1} & -c_{I3} \\ 0 & c_{R1} & c_{R3} & 0 & -c_{I2} \\ 0 & c_{I2} & 0 & c_{R1} & c_{R3} \\ 0 & c_{I1} & c_{I3} & 1 & c_{R2} \end{vmatrix} > 0$$

Lemma 3. *Let λ_i and μ_{ij} denote the eigenvalues of matrices $\bar{L}_{ff}$ and A_1-A_2 ($i=1,\dots,m$, $j=1,2,3$), respectively. Under Assumption 1–2, matrix A_1-A_2 is negative definite if and only if*

$$\begin{aligned}&\alpha^2\iota_2^2(\alpha\iota_1+\beta\iota_2)\mathrm{Re}(\lambda_i)(\mathrm{Re}(\lambda_i)^2+\mathrm{Im}(\lambda_i)^2)-\alpha\beta\iota_1\iota_2\mathrm{Re}(\lambda_i)^2-\frac{1}{2}(\alpha\iota_1+\beta\iota_2)^2\mathrm{Im}(\lambda_i)^2\\&-\frac{1}{2}\{(\alpha\iota_1+\beta\iota_2)^4\mathrm{Im}(\lambda_i)^4+4\alpha\beta\iota_1\iota_2(\alpha\iota_1+\beta\iota_2)^2\mathrm{Re}(\lambda_i)^2\mathrm{Im}(\lambda_i)^2\}^{\frac{1}{2}}>0\end{aligned}\tag{9}$$

for all complex eigenvalues λ_i and

$$\frac{\beta\iota_1}{\alpha^2\iota_1\iota_2+\alpha\beta\iota_2^2}<\min(\lambda_i)\tag{10}$$

for other real eigenvalues λ_i.

Proof. Let μ denote an eigenvalue of the matrix A_1-A_2. Then $\det(\mu I_{3m}-(A_1-A_2))=0$. Note that

$$\begin{aligned}\det(\mu I_{3m}-(A_1-A_2))&=\begin{vmatrix}\mu I_m & -I_m & \mathbf{0}_{m\times m}\\ \alpha\iota_1\bar{L}_{ff} & \mu I_m+\alpha\iota_2\bar{L}_{ff} & -I_m\\ \beta\iota_1\bar{L}_{ff} & \beta\iota_2\bar{L}_{ff} & \mu I_m\end{vmatrix}\\&=\left|\mu^3 I_m+\mu^2\alpha\iota_2\bar{L}_{ff}+\mu(\alpha\iota_1+\beta\iota_2)\bar{L}_{ff}+\beta\iota_1\bar{L}_{ff}\right|\\&=\prod_{i=1}^{m}(\mu^3+\mu^2\alpha\iota_2\lambda_i+\mu(\alpha\iota_1+\beta\iota_2)\lambda_i+\beta\iota_1\lambda_i)=0\end{aligned}\tag{11}$$

By Lemma 2, we can know that if eigenvalue λ_i is complex, all roots of equation $\mu^3+\mu^2\alpha\iota_2\lambda_i+\mu(\alpha\iota_1+\beta\iota_2)\lambda_i+\beta\iota_1\lambda_i=0$ have negative real parts if and only if the following inequalities hold:

$$\Delta_{1i}=\alpha\iota_2\mathrm{Re}(\lambda_i)>0\tag{12}$$

$$\Delta_{2i}=\begin{vmatrix}\alpha\iota_2\mathrm{Re}(\lambda_i) & \beta\iota_1\mathrm{Re}(\lambda_i) & -(\alpha\iota_1+\beta\iota_2)\mathrm{Im}(\lambda_i)\\ 1 & (\alpha\iota_1+\beta\iota_2)\mathrm{Re}(\lambda_i) & -\alpha\iota_2\mathrm{Im}(\lambda_i)\\ 0 & (\alpha\iota_1+\beta\iota_2)\mathrm{Im}(\lambda_i) & \alpha\iota_2\mathrm{Re}(\lambda_i)\end{vmatrix}>0\tag{13}$$

$$\Delta_{3i}=\begin{vmatrix}\alpha\iota_2\mathrm{Re}(\lambda_i) & \beta\iota_1\mathrm{Re}(\lambda_i) & 0 & -(\alpha\iota_1+\beta\iota_2)\mathrm{Im}(\lambda_i) & 0\\ 1 & (\alpha\iota_1+\beta\iota_2)\mathrm{Re}(\lambda_i) & 0 & -\alpha\iota_2\mathrm{Im}(\lambda_i) & -\beta\iota_1\mathrm{Im}(\lambda_i)\\ 0 & \alpha\iota_2\mathrm{Re}(\lambda_i) & \beta\iota_1\mathrm{Re}(\lambda_i) & 0 & -(\alpha\iota_1+\beta\iota_2)\mathrm{Im}(\lambda_i)\\ 0 & (\alpha\iota_1+\beta\iota_2)\mathrm{Im}(\lambda_i) & 0 & \alpha\iota_2\mathrm{Re}(\lambda_i) & \beta\iota_1\mathrm{Re}(\lambda_i)\\ 0 & \alpha\iota_2\mathrm{Im}(\lambda_i) & \beta\iota_1\mathrm{Im}(\lambda_i) & 1 & (\alpha\iota_1+\beta\iota_2)\mathrm{Re}(\lambda_i)\end{vmatrix}>0\tag{14}$$

It is easy to known that all eigenvalues λ_i have positive real parts under Assumption 1–2. Therefore, $\Delta_{1i}>0$ obviously holds. By some calculations,

$$\Delta_{2i}=\alpha^2\iota_2^2(\alpha\iota_1+\beta\iota_2)\mathrm{Re}(\lambda_i)(\mathrm{Re}(\lambda_i)^2+\mathrm{Im}(\lambda_i)^2)-\alpha\beta\iota_1\iota_2\mathrm{Re}(\lambda_i)^2-(\alpha\iota_1+\beta\iota_2)^2\mathrm{Im}(\lambda_i)^2\tag{15}$$

$$\Delta_{3i}=\beta\iota_1(\alpha\iota_1+\beta\iota_2)(\mathrm{Re}(\lambda_i)^2+\mathrm{Im}(\lambda_i)^2)\Delta_{2i}-\alpha\beta^2\iota_1^2\iota_2(\alpha\iota_1+\beta\iota_2)\mathrm{Re}(\lambda_i)^2(\mathrm{Re}(\lambda_i)^2+\mathrm{Im}(\lambda_i)^2)+\beta^3\iota_1^3\mathrm{Re}(\lambda_i)^3\tag{16}$$

Using Eq. (15), Eq. (16) can be further calculated as follows:

$$\begin{aligned}\Delta_{3i}=&\beta\iota_1(\alpha\iota_1+\beta\iota_2)(\mathrm{Re}(\lambda_i)^2+\mathrm{Im}(\lambda_i)^2)\Delta_{2i}-\frac{\beta^2\iota_1^2}{\alpha\iota_2}\mathrm{Re}(\lambda_i)(\Delta_{2i}+(\alpha\iota_1+\beta\iota_2)^2\mathrm{Im}(\lambda_i)^2)\\=&\frac{\beta\iota_1}{\alpha^2\iota_2{}^2\mathrm{Re}(\lambda_i)}\{\Delta_{2i}(\Delta_{2i}+(\alpha\iota_1+\beta\iota_2)^2\mathrm{Im}(\lambda_i)^2)-\alpha\beta\iota_1\iota_2(\alpha\iota_1+\beta\iota_2)^2\mathrm{Re}(\lambda_i)^2\mathrm{Im}(\lambda_i)^2\}\end{aligned}\tag{17}$$

Observing Eq. (17), $\Delta_{3i}>0$ is equivalent to

$$\Delta_{2i}{}^2+(\alpha\iota_1+\beta\iota_2)^2\mathrm{Im}(\lambda_i)^2\Delta_{2i}-\alpha\beta\iota_1\iota_2(\alpha\iota_1+\beta\iota_2)^2\mathrm{Re}(\lambda_i)^2\mathrm{Im}(\lambda_i)^2>0\tag{18}$$

Combining the solution of Eq. (17) and inequality $\Delta_{2i}>0$, condition (9) holds. If eigenvalue λ_i has zero imaginary part, condition (9) can be reduced to $(\alpha^2\iota_1\iota_2+\alpha\beta\iota_2^2)\lambda_i-\beta\iota_1>0$. Hence, $\mathrm{Re}(\mu_{ij})<0$ for any $i=1,\dots,m$, $j=1,2,3$ if and only if Eqs. (9) and (10) hold for all complex λ_i and other real λ_i, respectively. □

Give some constants $\gamma,\gamma^*,\kappa>0$ and let $\bar{\lambda}$ denote the maximum eigenvalue of real symmetric matrix $\bar{L}_{ff}^T\bar{L}_{ff}$. The following notations will be used in this section: $\sigma_{\max}=\max\{\sigma_i\}$, $\phi_{\max}=\max\{\phi_i\}$, $\gamma_{\min}=\min\{\gamma_i\}$, $b_0=\max\{1/(\rho_1-\rho_1\sigma_{\max}),1/(\rho_2-\rho_2\sigma_{\max}),\beta\sqrt{\bar{\lambda}}/\rho_3\}$, $b_1=m\sigma_{\max}(\rho_1+\rho_2)b_0$, $b_2=m\phi_{\max}b_0$, $h^*=(\gamma-\kappa\alpha_1b_1)/(\kappa\alpha_2+\kappa\alpha_3+\kappa\alpha_3b_1)$, $\sigma^*=\sup\{\sigma_{\max}|\gamma-\kappa\alpha_1b_1>0,\sigma_{\max}\in[0,1)\}$, $\alpha_1=\|A_2\|$, $\alpha_2=\|A_2A_1\|$, $\alpha_3=\|A_2A_2\|$, $\alpha_4=(\alpha_1b_2e^{\gamma^*h}\gamma^*+\alpha_3b_2e^{\gamma^*h}(e^{\gamma^*h}-1))/((\gamma-\gamma^*)\gamma^*)$, $\alpha_5=(\alpha_1b_1\gamma^*e^{\gamma^*h}+(\alpha_2+(\alpha_3+\alpha_3b_1)e^{\gamma^*h})(e^{\gamma^*h}-1))/((\gamma-\gamma^*)\gamma^*)$, $\alpha_6=(a_1b_2e^{\gamma_{\min}h}\gamma_{\min}+a_3b_2e^{\gamma_{\min}h}(e^{\gamma_{\min}h}-1))/((\gamma_{\min}-\gamma)\gamma_{\min})$, $\alpha_7=(a_1b_2e^{\gamma_{\min}h}\gamma_{\min}+a_3b_2e^{\gamma_{\min}h}(e^{\gamma_{\min}h}-1))/((\gamma_{\min}-\gamma^*)\gamma_{\min})$, $Z_1=\max\{\kappa\alpha_4/(1-\kappa\alpha_5),\kappa\|x(0)\|\}$, $Z_2=\max\{\kappa\alpha_6/(1-\kappa\alpha_5),\kappa\|x(0)\|+\kappa\alpha_6\}$, $Z_3=\max\{\kappa\alpha_7/(1-\kappa\alpha_5),\kappa\|x(0)\|+\kappa\alpha_7\}$.

Theorem 1. *Suppose Assumption 1–2 hold. Consider multi-agent systems (1)–(2) with control law (5) and the triggering instants are determined by the distributed event-triggered mechanism (6). The affine formation maneuver is achieved if the following conditions are satisfied:*

(1) Control gains ι_1, ι_2, α, β satisfy Eqs. (9) and (10) for all complex eigenvalues λ_i and for other real eigenvalues λ_i, respectively.
(2) For some $\rho_1 > 0$, $\rho_2 > 0$, $\rho_3 > 0$, there exist $\sigma_i \in (0, \sigma^*)$. $\phi_i > 0$ and $\gamma_i > 0$ can be arbitrary.
(3) The sampling period $h \in (0, h^*)$.

Proof. Let $\tau(t) = t - lh$ for any $t \in [lh, lh + h)$, and then Eq. (8) can be rewritten as

$$\dot{x}(t) = (A_1 \otimes I_d)x(t) - (A_2 \otimes I_d)x(t - \tau(t)) + (A_2 \otimes I_d)e(t - \tau(t)) \tag{19}$$

Applying the Newton–Leibnitz formula for Eq. (19), we have

$$\begin{aligned}\dot{x}(t) =&((A_1 - A_2) \otimes I_d)x(t) + (A_2 \otimes I_d)e(t - \tau(t)) + (A_2 \otimes I_d)\int_{t-\tau(t)}^{t} \{(A_1 \otimes I_d)x(s) - (A_2 \otimes I_d)(x(s - \tau(s))\\ &-e(s - \tau(s)))\}\, ds\end{aligned} \tag{20}$$

The solution of Eq. (20) is given by

$$\begin{aligned}x(t) =&e^{((A_1-A_2)\otimes I_d)t}x(0) + \int_0^t e^{((A_1-A_2)\otimes I_d)(t-s)}\{(A_2 \otimes I_d)e(s - \tau(s)) + (A_2 \otimes I_d)\int_{s-\tau(s)}^{s} ((A_1 \otimes I_d)x(z)\\ &- (A_2 \otimes I_d)(x(z - \tau(z)) - e(z - \tau(z))))dz\}ds\end{aligned} \tag{21}$$

By Lemma 3, it is known that matrix $A_1 - A_2$ is negative definite. Hence, there exist constants $\kappa \geq 1$ and $\gamma > 0$ such that

$$\|x(t)\| \leq \kappa e^{-\gamma t}\|x(0)\| + \int_0^t \kappa e^{-\gamma(t-s)}\{\alpha_1 \|e(s - \tau(s))\| + \int_{s-\tau(s)}^{s} (\alpha_2 \|x(z)\| + \alpha_3 \|x(z - \tau(z))\| + \alpha_3 \|e(z - \tau(z))\|)dz\}ds \tag{22}$$

The triggering condition (6) enforces that

$$\rho_1\|e_{pi}(lh)\| + \rho_2\|e_{vi}(lh)\| + \rho_3\|e_{\xi i}(lh)\| \leq \sigma_i(\rho_1\|x_{pi}(t_k^i h)\| + \rho_2\|x_{vi}(t_k^i h)\|) + \phi_i e^{-\gamma_i lh} \tag{23}$$

which means

$$(1 - \sigma_{\max})(\rho_1 \left\|e_{pi}(lh)\right\| + \rho_2 \|e_{vi}(lh)\|) + \rho_3 \left\|e_{\xi i}(lh)\right\| \leq \sigma_{\max}\left(\rho_1 \left\|x_p(lh)\right\| + \rho_2 \|x_v(lh)\|\right) + \phi_{\max}e^{-\gamma_{\min}lh} \tag{24}$$

Notice that

$$\left\|e_c(lh)\right\| = \beta\sqrt{e_{\xi}^T(lh)(\bar{L}_{ff}^T\bar{L}_{ff} \otimes I_d)e_{\xi}(lh)} \leq \beta\sqrt{\bar{\lambda}}\left\|e_{\xi}(lh)\right\| \tag{25}$$

Applying Eqs. (24)–(25), we can derive

$$\begin{aligned}\|e(lh)\| \leq& \sum_{i=1}^{m}(\left\|e_{pi}(lh)\right\| + \|e_{vi}(lh)\|) + \left\|e_c(lh)\right\| \leq \sum_{i=1}^{m}(\left\|e_{pi}(lh)\right\| + \|e_{vi}(lh)\| + \beta\sqrt{\bar{\lambda}}\left\|e_{\xi i}(lh)\right\|)\\ \leq& b_0 m(\sigma_{\max}(\rho_1 \left\|x_p(lh)\right\| + \rho_2 \|x_v(lh)\|) + \phi_{\max}e^{-\gamma_{\min}lh}) \leq b_0 m(\sigma_{\max}(\rho_1 + \rho_2)\|x(lh)\| + \phi_{\max}e^{-\gamma_{\min}lh})\end{aligned} \tag{26}$$

which ensures that the following inequality holds:

$$\|e(lh)\| \leq b_1 \|x(lh)\| + b_2 e^{-\gamma_{\min}lh} \tag{27}$$

Substituting Eq. (27) into Eq. (22), we can obtain

$$\begin{aligned}\|x(t)\| \leq& \kappa e^{-\gamma t}\|x(0)\| + \int_0^t \kappa e^{-\gamma(t-s)}\alpha_1 b_1 \|x(s - \tau(s))\|\, ds + \int_0^t \kappa e^{-\gamma(t-s)}\int_{s-h}^{s} (\alpha_2 \|x(z)\| + \alpha_3 \|x(z - \tau(z))\|\\ &+ \alpha_3 b_1 \|x(z - \tau(z))\|)dz ds + \int_0^t \kappa e^{-\gamma(t-s)}\alpha_1 b_2 e^{-\gamma_{\min}(s-h)}ds + \int_0^t \kappa e^{-\gamma(t-s)}\alpha_3 b_2 \int_{s-h}^{s} e^{-\gamma_{\min}(z-h)}dz ds\end{aligned} \tag{28}$$

In the next, it will be proved that there exist $\eta > 1$ and $\gamma^* \in (0, \gamma)$ satisfying

$$\frac{\kappa\alpha_1 b_1\gamma^* e^{\gamma^* h} + \kappa(\alpha_2 + (\alpha_3 + \alpha_3 b_1)e^{\gamma^* h})(e^{\gamma^* h} - 1)}{(\gamma - \gamma^*)\gamma^*} < 1 \tag{29}$$

such that for any $t \geq 0$

$$\|x(t)\| < \eta Z e^{-\gamma^* t} \triangleq \delta(t) \tag{30}$$

where

$$Z = \begin{cases} Z_1, \gamma > \gamma_{\min} \\ Z_2, \gamma < \gamma_{\min} \\ Z_3, \gamma = \gamma_{\min} \end{cases}$$

First, the existence of γ^* will be proved. Define function $\chi(\gamma^*) = \kappa\alpha_1 b_1\gamma^* e^{\gamma^* h} + \kappa(\alpha_2 + (\alpha_3 + \alpha_3 b_1)e^{\gamma^* h})(e^{\gamma^* h} - 1) - (\gamma - \gamma^*)\gamma^*$. It can be easily derived that $\chi(0) = 0$ and $\dot{\chi}(0) = \kappa\alpha_1 b_1 + \kappa(\alpha_2 + \alpha_3 + \alpha_3 b_1)h - \gamma$. $\sigma_i \in (0, \sigma^*)$ means $\kappa\alpha_1 b_1 - \gamma < 0$. Then $\dot{\chi}(0) < 0$ from $h \in (0, h^*)$. Hence there must be $\gamma^* \in (0, \gamma)$ such that $\chi(\gamma^*) < 0$, which implies Eq. (29) holds.

Second, Eq. (30) will be proved by contradiction. Suppose Eq. (30) is not true, and then there exists $t^* > 0$ such that

$$\|x(t^*)\| = \eta Z e^{-\gamma^* t^*} = \delta(t^*), \tag{31}$$

and for $0 \le t < t^*$,

$$\|x(t)\| < \delta(t). \tag{32}$$

By Eq. (28) and Eqs. (31)–(32), we obtain

$$\begin{aligned}\delta(t^*) <& \eta\kappa\{e^{-\gamma t^*}\|x(0)\| + a_1 b_1 e^{\gamma^* h} Z e^{-\gamma t^*}\int_0^{t^*} e^{-(\gamma^*-\gamma)s} ds + (a_2 + (a_3 + a_3 b_1)e^{\gamma^* h}) Z e^{-\gamma t^*}\int_0^{t^*} e^{\gamma s}\int_{s-h}^{s} e^{-\gamma^* z} dz ds \\ &+ a_1 b_2 e^{\gamma_{\min} h} e^{-\gamma t^*}\int_0^{t^*} e^{-(\gamma_{\min}-\gamma)s} ds + a_3 b_2 e^{\gamma_{\min} h} e^{-\gamma t^*}\int_0^{t^*} e^{\gamma s}\int_{s-h}^{s} e^{-\gamma_{\min} z} dz ds\}\end{aligned} \tag{33}$$

The calculation of Eq. (32) will be further divided into three cases.

Case 1: $\gamma > \gamma_{\min}$.

Choose $\gamma^* = \gamma_{\min}$ and then Eq. (33) can be further written as

$$\delta(t^*) = \|x(t^*)\| < \eta e^{-\gamma^* t^*}\kappa(\alpha_4 + Z_1\alpha_5) + \eta e^{-\gamma t^*}(\kappa\|x(0)\| - \kappa(\alpha_4 + Z_1\alpha_5)) \tag{34}$$

If $Z_1 = \kappa\alpha_4/(1 - \kappa\alpha_5)$, $\kappa\|x(0)\| - \kappa(\alpha_4 + Z_1\alpha_5) \le 0$ holds and then by Eq. (34) we obtain

$$\delta(t^*) < \eta\kappa(\alpha_4 + Z_1\alpha_5)e^{-\gamma^* t^*} = \eta Z_1 e^{-\gamma^* t^*} = \delta(t^*) \tag{35}$$

If $Z_1 = \kappa\|x(0)\|$ and $1 - \kappa\alpha_5 > 0$, $\kappa\|x(0)\| - \kappa(\alpha_4 + Z_1\alpha_5) \ge 0$ holds and then

$$\delta(t^*) < \eta\kappa\|x(0)\| e^{-\gamma^* t^*} = \eta Z_1 e^{-\gamma^* t^*} = \delta(t^*) \tag{36}$$

Case 2: $0 < \gamma < \gamma_{\min}$.

Choose γ^* satisfying $\gamma^* < \gamma$, and then

$$\delta(t^*) = \|x(t^*)\| < \eta e^{-\gamma t^*}\kappa(\|x(0)\| - Z_2\alpha_5) + \eta e^{-\gamma^* t^*}\kappa(Z_2\alpha_5 + \alpha_6) \tag{37}$$

If $Z_2 = \kappa\alpha_6/(1 - \kappa\alpha_5)$, $\kappa\|x(0)\| - \kappa Z_2\alpha_5 \le 0$ holds, and then by Eq. (37) we derive

$$\delta(t^*) < \eta e^{-\gamma^* t^*}\kappa(Z_2\alpha_5 + \alpha_6) = \eta Z_2 e^{-\gamma^* t^*} = \delta(t^*) \tag{38}$$

If $Z_2 = \kappa\|x(0)\| + \kappa\alpha_6$ and $1 - \kappa\alpha_5 > 0$, $\kappa\|x(0)\| - \kappa Z_2\alpha_5 \ge 0$ holds, and then

$$\delta(t^*) < \eta e^{-\gamma^* t^*}(\kappa\|x(0)\| + \kappa\alpha_6) = \eta Z_2 e^{-\gamma^* t^*} = \delta(t^*) \tag{39}$$

Case 3: $0 < \gamma = \gamma_{\min}$.

Choose γ^* satisfying $\gamma^* < \gamma$, and then

$$\delta(t^*) < \eta\kappa\{\|x(0)\| e^{-\gamma t^*} + Z_3\alpha_5(e^{-\gamma^* t^*} - e^{-\gamma t^*}) + \alpha_7(\gamma - \gamma^*)t^* e^{-\gamma t^*}\} \tag{40}$$

holds. Applying inequality $(\gamma - \gamma^*)t^* < e^{(\gamma-\gamma^*)t^*}$ into Eq. (40), we derive

$$\delta(t^*) = \|x(t^*)\| < \eta e^{-\gamma t^*}\kappa(\|x(0)\| - Z_3\alpha_5) + \eta e^{-\gamma^* t^*}\kappa(Z_3\alpha_5 + \alpha_7) \tag{41}$$

If $Z_3 = \kappa\alpha_7/(1 - \kappa\alpha_5)$, $\kappa\|x(0)\| - \kappa Z_3\alpha_5 \le 0$ holds, and then by Eq. (41) we can derive

$$\delta(t^*) < \eta e^{-\gamma^* t^*}\kappa(Z_3\alpha_5 + \alpha_7) = \eta Z_3 e^{-\gamma^* t^*} = \delta(t^*) \tag{42}$$

If $Z_3 = \kappa\|x(0)\| + \kappa\alpha_7$ and $1 - \kappa\alpha_5 > 0$, $\kappa\|x(0)\| - \kappa Z_3\alpha_5 \ge 0$ holds, and then

$$\delta(t^*) < \eta e^{-\gamma^* t^*}(\kappa\|x(0)\| + \kappa\alpha_7) = \eta Z_3 e^{-\gamma^* t^*} = \delta(t^*) \tag{43}$$

The contradiction of any one of Eq. (35), Eq. (36), Eq. (38), Eq. (39), Eq. (42) and (43) indicates that Eq. (30) is valid for any $\gamma, \gamma_{\min} > 0$. Let $\eta \to 1$, and we can obtain

$$\|x(t)\| < Z e^{-\gamma^* t} \tag{44}$$

for $t \ge 0$. Eq. (44) implies $x(t)$ will exponentially converge to zero. Therefore, the affine formation maneuver is achieved. □

Remark 2. According to the event-triggered mechanism (6), it can be known that the triggering frequency of agent i will get lower as γ_i gets smaller and ϕ_i gets bigger. And the proof process of Eq. (44) in Theorem 1 means that if $\gamma_{min} < \gamma$, the convergence rate of error system (8) will get slower while γ_{min} gets smaller and ϕ_{max} gets bigger for some initial value $\|x(0)\|$. Thus, the triggering frequency performance and convergence performance of dynamic formation proposed in this paper can be mostly balanced by selecting appropriate values of parameters γ_i and ϕ_i.

Remark 3. The event-triggered mechanism based on sampled-data makes the lengths of all triggering intervals greater than or equal to the sampling period. In scheme (6), it is obvious that there does not exist Zeno behavior, that is, an infinite number of triggering will not occur within a limited time.

Remark 4. When event-triggered function contains an exponential function term about t like Eq. (6), analytic method and Lyapunov function method are used in literature [29,35,36] and literature [37–39], respectively. The proof process of Theorem 1 is similar to [29,35,36]. However, different from literature [29,35,36], Theorem 1 indicates that the relationship between γ and $\gamma_{\min}$ in value size does not determine whether the dynamic formation converges or not while using the triggering condition with an exponential term, which is consistent with the results in [37–39]. Meanwhile, sampled-data-based event-triggered mechanism can be regarded as the event-triggered mechanism with time delay like [35]. To achieve the affine formation maneuver, the triggering control strategy does not allow the sampling interval to be arbitrary, which results in the formal difference between the sampling interval constraint or the delay constraint given in Theorem 1 and literature [35]. As a result, the analysis strategy of Theorem 1 can further improve the results in [29,35,36]. Notice that the significant differences between our work and [35] are the analysis process and the form of control scheme where the control law and event-triggered function contain an integral term in this paper, which can make followers track leaders moving with constant acceleration and multi-agent systems achieve affine formation maneuver.

Remark 5. In fact, the event-triggered affine formation maneuver problem can be regarded as an event-triggered containment problem for multi-agent systems. But the type of triggering control law is proportional for containment problem in the existing literature [40–43], where the control input of leaders is considered as zero like [40–42] or all the states information of leader dynamics is known by followers like [43]. Different from [40–43], the setting of constant acceleration in the leader dynamic (2) means that the control input or the external input signal of leaders is nonzero, which leads to the integral term being considered in the control law (5) to ensure zero tracking errors for followers. The compensation item appears not only in the controller (5) but also in the event-triggered function (7) and makes the stability analysis of the proposed algorithms different from that in [40–43]. The analysis strategies displayed in this paper can be referenced for addressing distributed event-triggered containment scheme problem with proportional-integral controller.

4. Self-triggered affine formation maneuver algorithm

In the distributed event-triggered mechanism (6), agent i still needs to continuously measure the relative states between itself and its neighbors and continuously detect local events. Hence, a self-triggered algorithm will be proposed based on the event-triggered mechanism (6), which can further reduce the frequency of measurement for relative states and detection for triggering condition.

Assume that all followers already know the accelerations of neighbor leaders before the movement starts. In the non-triggering interval $(t_k^i h, t_{k+1}^i h)$, denote the triggering time of all neighbors of agent i by $t_{k_i}^{j_1} h < t_{k_i}^{j_2} h < \cdots < t_{k_i}^{j_s} h < \cdots$, and let $t_{k_i}^{j_0} h = t_k^i h$. The self-triggered function $\bar{f}_i(t)$ can be designed as

$$\bar{f}_i(t) = \bar{g}_i(t) - \sigma_i(\rho_1 \left\| x_{pi}(t_k^i h) \right\| + \rho_2 \left\| x_{vi}(t_k^i h) \right\|) - \phi_i e^{-\gamma_i t} \tag{45}$$

where for $t \in (t_{k_i}^{j_s} h, t_{k_i}^{j_{s+1}} h]$,

$$\bar{g}_i(t) = \begin{cases} \Phi_i(t_{k_i}^{j_s} h)(e^{t - t_{k_i}^{j_s} h} - 1), s = 0 \\ e^{t - t_{k_i}^{j_s} h}(\Phi_i(t_{k_i}^{j_s} h) + \bar{g}_i(t_{k_i}^{j_s} h)) - \Phi_i(t_{k_i}^{j_s} h), s > 0 \end{cases}$$

$$\Phi_i(t) = \rho_1 \left\| x_{vi}(t_k^i h) \right\| + \rho_2 \| d_i \sum_{j=1}^{n} w_{ij} u_i(t_k^i h) - d_i \sum_{j=1}^{m} w_{ij} u_j(t) - d_i \sum_{j=m+1}^{n} w_{ij} a_j \| + \rho_3 \left\| \iota_1 x_{pi}(t_k^i h) + \iota_2 x_{vi}(t_k^i h) \right\|$$

Knowing the current triggering instant $t_k^i h$ and the last neighbor triggering instant $t_{k_i}^{j_s} h$, the next triggering instant of follower i is determined by

$$t_{k+1}^i h = inf \{ l : lh > t_k^i h, \bar{f}_i(lh) \geq 0 \} \tag{46}$$

In the self-triggered mechanism (46), agent i will measure the relative states between itself and its neighbors to obtain $x_{pi}(t_k^i h)$, $x_{vi}(t_k^i h)$ and $\xi_i(t_k^i h)$ at each triggering time $t_k^i h$, which will be send to its neighbors simultaneously through network transmission and then control input $u_i(t)$ will be updated immediately. Although communication network is additionally operated in scheme (46), the frequency of measurement for each agent is reduced and is same as that of network transmission. Notice that the flow of measurement actions between adjacent agents finally constitutes measurement network. Thus, it can be pointed that the times of information interaction involving non-local states will diminish under the proposed self-triggered algorithm.

Remark 6. Applying the self-triggered mechanism (46), agent i will first calculate the next triggering instant $\bar{t}_k^i h$ according to the last information at $t_k^i h$. If no neighbor of agent i is triggered during $(t_k^i h, \bar{t}_k^i h)$, then let $t_{k+1}^i h = \bar{t}_k^i h$; otherwise, update the parameters of self-triggered function $\bar{f}_i(t)$ and recalculate $\bar{t}_k^i h$ at each last triggering instant of neighbors for agent i; repeat these steps until the value of $t_{k+1}^i h$ is given.

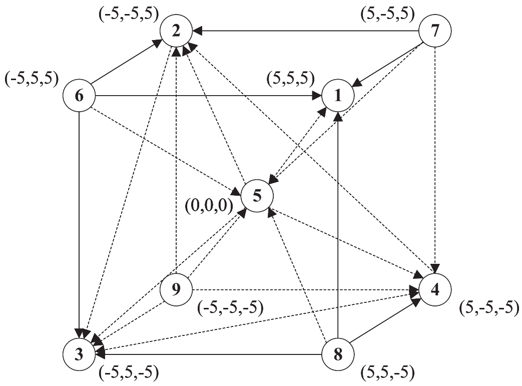

Fig. 1. The directed network topology and the nominal configuration.

Remark 7. If all followers only know the maximum acceleration of leaders, then the second item of $\Phi_i(t)$ can be replaced by $\rho_2\|d_i \sum_{j=1}^{n} w_{ij}u_i(t_k^i h) - d_i \sum_{j=1}^{m} w_{ij}u_j(t)\| + \max_{i\in\mathcal{V}_l}(\|a_i\|)\|\sum_{j=m+1}^{n} w_{ij}\|$. At this time, $\Phi_i(t)$ in Eq. (45) is amplified, which leads to a higher triggering frequency.

Theorem 2. *Suppose Assumption 1–2 hold. Consider multi-agent systems (1)–(2) with control law (5) and the triggering instants are determined by the self-triggered mechanism (46). If all conditions of Theorem 1 hold, then the affine formation maneuver is achieved.*

Proof. Let $g_i(t) = \rho_1 \left\|e_{pi}(t)\right\| + \rho_2 \left\|e_{vi}(t)\right\| + \rho_3 \left\|e_{\xi i}(t)\right\|$. For any $t \in [t_k^i h, t_{k+1}^i h)$, take the derivative of $g_i(t)$ and we have

$$\dot{g}_i(t) \le \rho_1 \left\|\dot{e}_{pi}(t)\right\| + \rho_2 \left\|\dot{e}_{vi}(t)\right\| + \rho_3 \left\|\dot{e}_{\xi i}(t)\right\| \le g_i(t) + \Phi_i(t) \tag{47}$$

If no neighbor of agent i is triggered during $(t_k^i h, t_{k+1}^i h)$, that is $s = 0$, it can be deduced from Eq. (47) that

$$\dot{g}_i(t) \le g_i(t) + \Phi_i(t_k^i h) \tag{48}$$

which can be further calculated as follows:

$$g_i(t) \le \Phi_i(t_k^i h)(e^{t-t_k^i h} - 1) \tag{49}$$

If there are exactly $s > 0$ neighbors of agent i triggered during $(t_k^i h, t_{k+1}^i h)$, Eq. (47) can be solved as

$$g_i(t) \le \Phi_i(t_{k_i}^{j_s} h)(e^{t-t_{k_i}^{j_s} h} - 1) + \Phi_i(t_{k_i}^{j_{s-1}} h)(e^{t-t_{k_i}^{j_{s-1}} h} - e^{t-t_{k_i}^{j_s} h}) + \cdots + \Phi_i(t_k^i h)(e^{t-t_k^i h} - e^{t-t_{k_i}^{j_1} h}) \tag{50}$$

According to Eqs. (49)–(50), $g_i(t) \le \bar{g}_i(t)$ holds. Obviously, if $\bar{f}_i(t) < 0$, $f_i(t) < 0$ holds. The rest of proof is same with the proof of Theorem 1. □

5. Simulation

In this section, we will provide simulation examples to illustrate effectiveness of the proposed algorithms.

In three-dimensional space, consider multi-agent systems composed of 5 followers and 4 leaders which are labeled as 1, 2, ⋯, 9. The coordinate axis of three-dimensional space is represented by X axis, Y axis and Z axis. The network topology and nominal configuration are shown in Fig. 1. And the corresponding Laplacian matrix blocks are as follows:

$$\bar{L}_{ff} = \begin{bmatrix} 0.5 & 0 & 0 & 0 & 1 \\ 0 & 0.8 & 0 & 0.6 & 0.4 \\ 0 & 0.15 & 1 & 0.2 & 1.3 \\ 0 & 0 & 0.1 & 0.8 & 1.4 \\ 0.1 & 0 & 0 & 0 & 2.2 \end{bmatrix}, \quad \bar{L}_{fl} = \begin{bmatrix} -0.5 & -0.5 & -0.5 & 0 \\ -0.2 & -0.8 & 0 & -0.8 \\ -0.8 & 0 & -0.85 & -1 \\ 0 & -0.7 & -0.8 & -0.8 \\ -0.6 & -0.6 & -0.6 & -0.5 \end{bmatrix}.$$

The dynamics (2) of leaders can be described as 2th-order polynomial trajectories and decide affine transformations of the overall formation. Therefore, based on the nominal formation shown in Fig. 1, an ideal affine transformation is designed as $(A^*(t), b^*(t)) = (A_a t^2 + A_v t + A_p, b_a t^2 + b_v t + b_p)$, where $A_p = [A_{pX}, A_{pY}, A_{pZ}]^T$, $A_{pX} = [0.9529, -0.5066, -0.1277]^T$, $A_{pY} = [0.3012, 1.0413, -0.1206]^T$, $A_{pZ} = [0.3166, 0.9977, 1.9761]^T$, $A_v = diag(0, -0.6, 0.2)$, $A_a = diag(0, 0.02, -0.025)$, $b_p = [5, 3.3, 0.02]^T$, $b_v = [1, 0.2, 0.05]^T$ and $b_a = [0.2, 0.01, -0.01]^T$. Notice that this affine transformation includes translation and scaling transformations with certain accelerations, and rotation and shearing transformations with given magnitudes. The initial positions of followers are given by $p_1(0) = [3.3, 4.8, 0]^T$, $p_2(0) = [1.1, -2, 0]^T$, $p_3(0) = [-0.9, 3.8, 0]^T$, $p_4(0) = [6.5, 0.1, 0]^T$ and $p_5(0) = [2.5, 1.6, 0]^T$; the initial values of velocities, control inputs and auxiliary states for follower i are $v_i(0) = [0.1, 0, 0]^T$, $u_i(0) = [0, 0, 0]^T$ and $\xi_i(0) = [0, 0, 0]^T$, respectively. In order to satisfy all

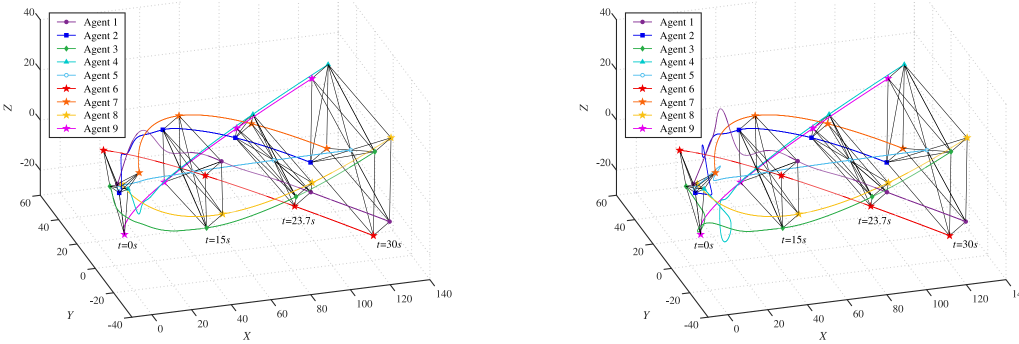

(a) Under the event-triggered algorithm (b) Under the self-triggered algorithm

Fig. 2. The motion trajectories of each agent.

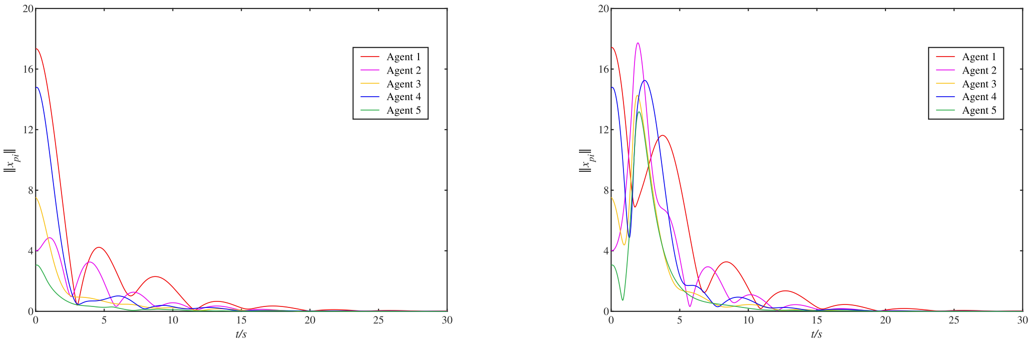

(a) Under the event-triggered algorithm (b) Under the self-triggered algorithm

Fig. 3. The norm of position tracking error $x_p(t)$ for followers.

conditions of Theorems 1 and 2, choose control gains $\iota_1 = 1$, $\iota_2 = 1.7$, $\alpha = 1$, $\beta = 0.3$, triggering parameters $\rho_1 = \rho_2 = \rho_3 = 1$, $\phi_i = 3$, $\gamma_i = 0.2$, $\sigma_i = 0.001$, and sampling period $h = 0.005$. The simulation time interval is set to 0 to 30 s.

The simulation results are shown in Fig. 2–6 under the event-triggered and self-triggered algorithms proposed in this paper. The motion trajectories of agents are depicted in Fig. 2, where real configuration and the network topologies without direction at $t = 0s, 15s, 23.7s, 30$ s are also marked by shape symbols and black lines. Fig. 3 shows the evolution of the norm of position tracking error for each follower. Observing Fig. 2 and Fig. 3, it is known that the time-varying configuration of 9 agents will converge into the affine image space of nominal configuration as time goes, which indicates that affine formation maneuver for multi-agent system (1)–(2) is achieved under the event-triggered and self-triggered algorithms. The value jumps of control input trajectories shown in Fig. 4 correspond to the triggering intervals for each follower in Fig. 5 and Fig. 6. The minimum and maximum triggering intervals for sampling mode are both 0.005 s. For event-triggered mode, the minimum and maximum triggering intervals of all followers are 0.065 s and 1.965 s. For self-triggered mode, these two intervals are 0.01 s and 1.75 s. These interval values and Fig. 4–6 mean low frequency triggering times and indicate that the controller update times of followers are effectively reduced under both event-triggered and self-triggered algorithms.

To further compare the work performances of the event-triggered algorithm and self-triggered one proposed in this paper, Tables 1 and 2 record the times of triggering, controller update, measurement, and network transmission of each follower under the corresponding algorithms. Setting the same parameters, it can be known that the measurement times of relative states and triggering detection times are smaller while the triggering times and controller update times of each other are similar, and the network transmission with a low frequency is added to support the realization for the self-triggering strategy. Finally, the resources of information interaction and calculation are efficiently saved for the affine formation maneuver problem.

As a result, the effectiveness of the proposed triggering algorithms in this paper is verified through above simulations.

6. Conclusion

This paper studied the distributed event-triggered and self-triggered strategies for affine formation maneuver of second-order multi-agents based on sampled-data. The proposed triggering mechanisms extended the work reported in [17] for affine formation maneuver, where the controller is proportional-integral type for multiple moving leaders with constant accelerations. As a result, the frequencies of information interaction and controller update are significantly reduced. Nevertheless, the setting of constant

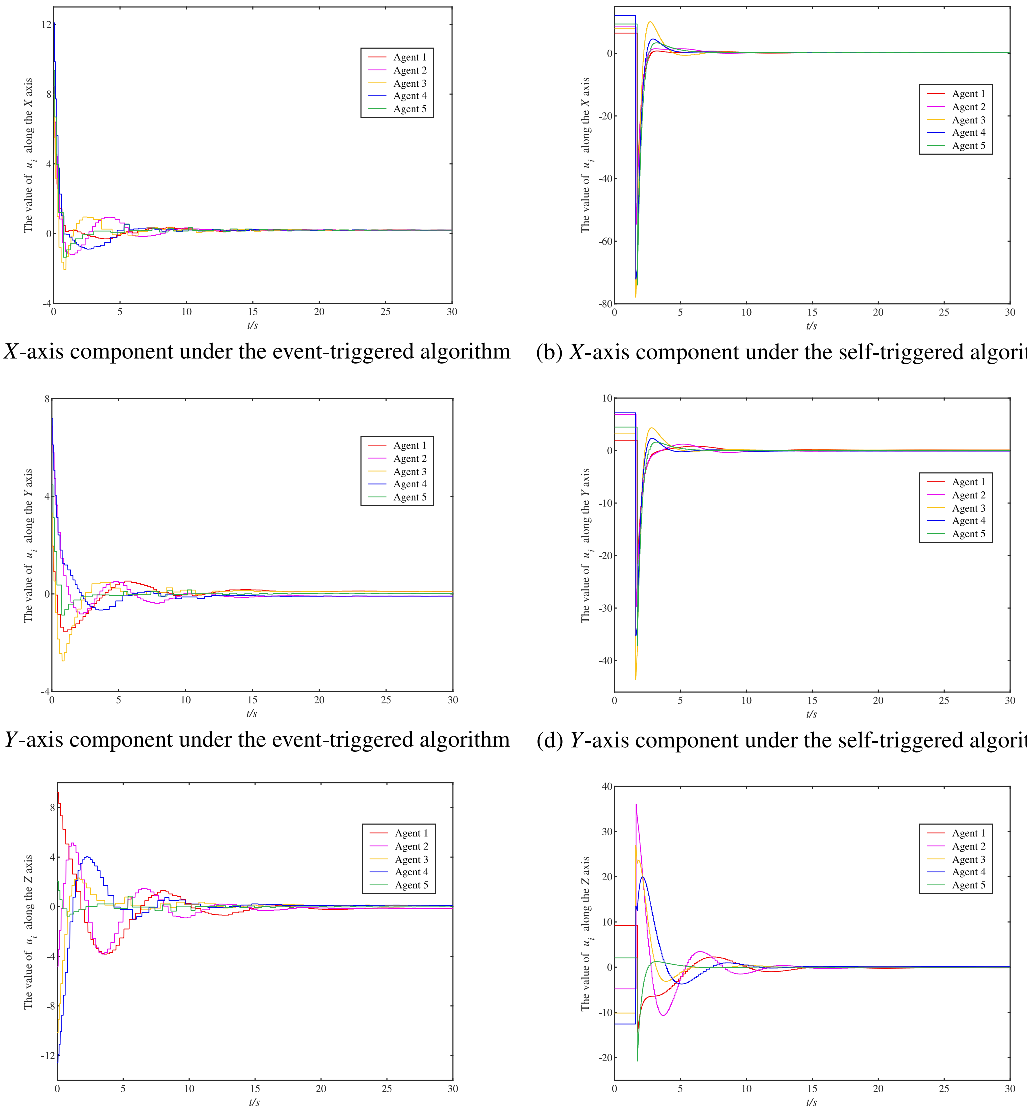

(a) X-axis component under the event-triggered algorithm (b) X-axis component under the self-triggered algorithm

(c) Y-axis component under the event-triggered algorithm (d) Y-axis component under the self-triggered algorithm

(e) Z-axis component under the event-triggered algorithm (f) Z-axis component under the self-triggered algorithm

Fig. 4. The control inputs for followers.

Table 1
Work performances under the event-triggered algorithm.

Agent	1	2	3	4	5	Total
Triggering/Controller update times	101	82	54	62	45	344
Triggering detection times	6000	6000	6000	6000	6000	30 000
Measurement times	6000	6000	6000	6000	6000	30 000
Network transmission times	0	0	0	0	0	0

Table 2
Work performances under the self-triggered algorithm.

Agent	1	2	3	4	5	Total
Triggering/Controller update times	173	169	141	152	112	747
Triggering detection times	275	407	526	386	275	1869
Measurement times	173	169	141	152	112	747
Network transmission times	173	169	141	152	112	747

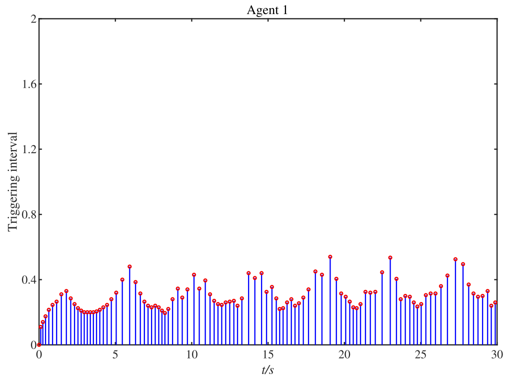

(a) The case of agent 1

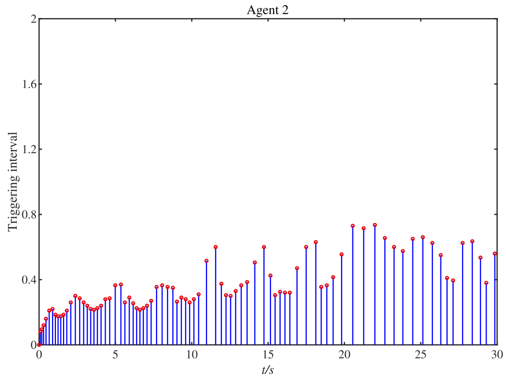

(b) The case of agent 2

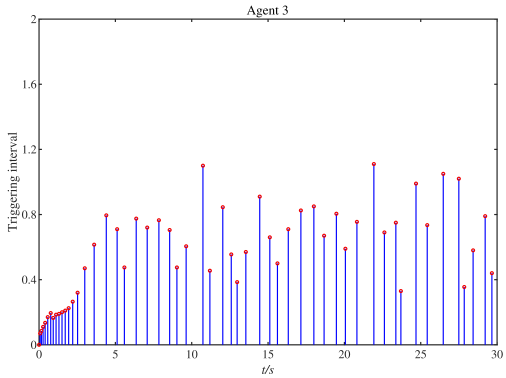

(c) The case of agent 3

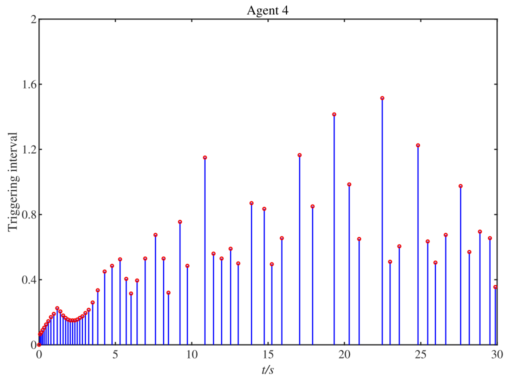

(d) The case of agent 4

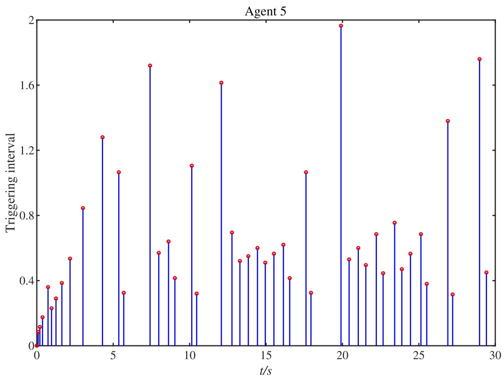

(e) The case of agent 5

Fig. 5. The triggering intervals for followers under the event-triggered algorithm.

accelerations for leaders will lead to only one formation maneuver scheme unless any constant acceleration of leaders is changed, and the selection pattern of algorithm parameters is centralized, which may limit practical application of the proposed algorithm. Therefore, future research will focus on introducing more effective triggering control scheme for affine formation maneuver considering time-varying acceleration leaders, and designing a fully distributed event-triggered maneuver control. In addition, it should be pointed that the directed topology design for $d+1$-rooted networks mentioned in Section 2.1 may be temporarily blank and is necessary.

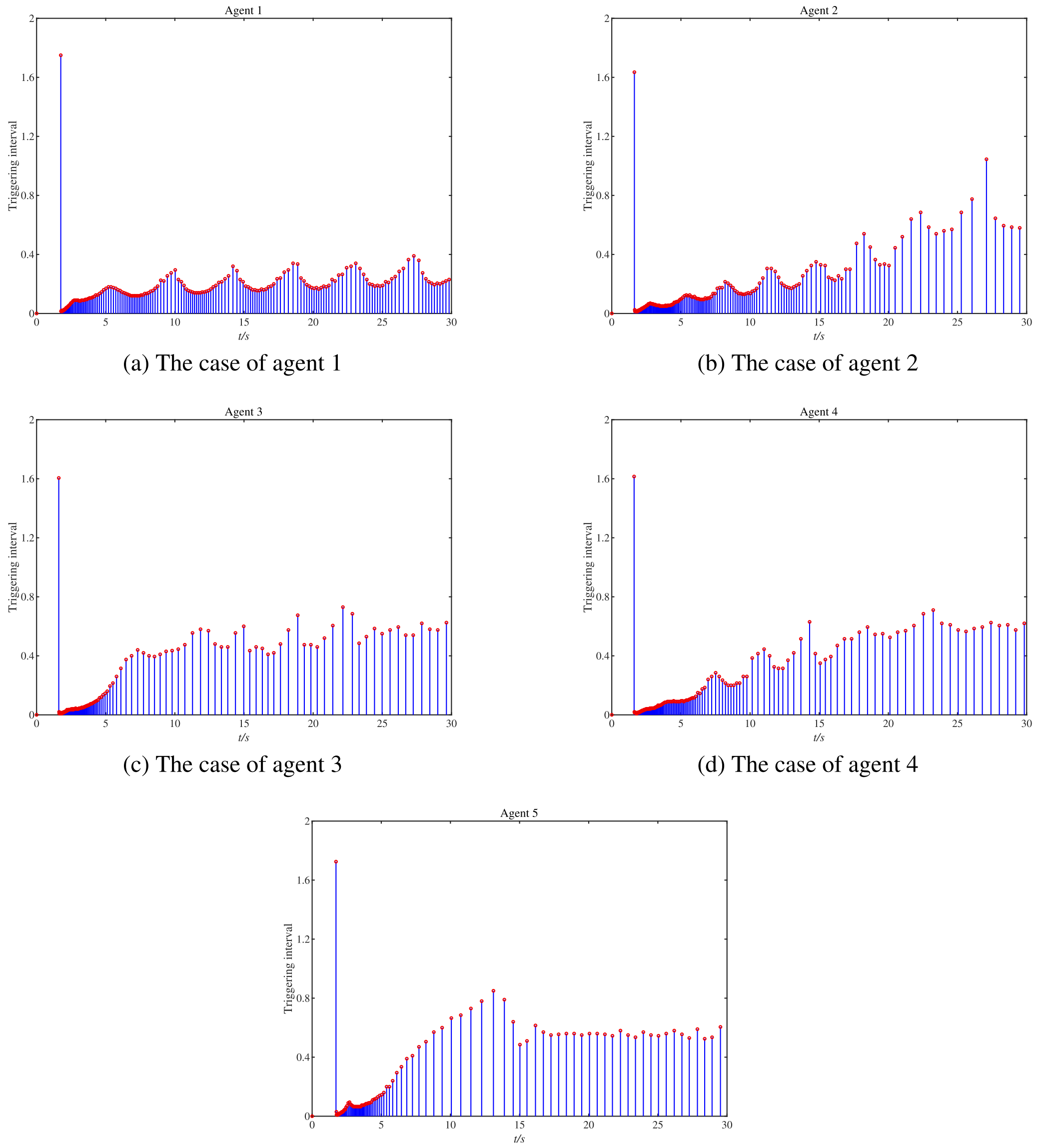

(a) The case of agent 1

(b) The case of agent 2

(c) The case of agent 3

(d) The case of agent 4

(e) The case of agent 5

Fig. 6. The triggering intervals for followers under the self-triggered algorithm.

Declaration of competing interest

The authors declare that they have no known competing financial interests or personal relationships that could have appeared to influence the work reported in this paper.

Acknowledgments

This work was supported by the National Natural Science Foundation of China (No. 61903301, 61933010).

References

[1] X. Dong, G. Hu, Time-varying formation control for general linear multi-agent systems with switching directed topologies, Automatica 73 (2016) 47–55, http://dx.doi.org/10.1016/j.automatica.2016.06.024.

[2] X. Dong, G. Hu, Time-varying formation tracking for linear multiagent systems with multiple leaders, IEEE Trans. Automat. Control 62 (7) (2017) 3658–3664, http://dx.doi.org/10.1109/TAC.2017.2673411.

[3] Y. Zhao, Q. Duan, G. Wen, D. Zhang, B. Wang, Time-varying formation for general linear multiagent systems over directed topologies: A fully distributed adaptive technique, IEEE Trans. Syst., Man, Cybern., Syst. 51 (1) (2021) 532–541, http://dx.doi.org/10.1109/TSMC.2018.2877818.
[4] Y. Cai, H. Zhang, Y. Wang, Z. Gao, Q. He, Adaptive bipartite fixed-time time-varying output formation-containment tracking of heterogeneous linear multiagent systems, IEEE Trans. Neural Netw. Learn. Syst. 33 (9) (2022) 4688–4698, http://dx.doi.org/10.1109/TNNLS.2021.3059763.
[5] T.-M. Nguyen, Z. Qiu, T.H. Nguyen, M. Cao, L. Xie, Persistently excited adaptive relative localization and time-varying formation of robot swarms, IEEE Trans. Robot. 36 (2) (2020) 553–560, http://dx.doi.org/10.1109/TRO.2019.2954677.
[6] J. Zhou, R. Huang, H.Q. Huang, Manoeuvrable multi-agent formation control via time-varying flocking and iterative learning tracking, Internat. J. Systems Sci. 52 (12) (2021) 2460–2479, http://dx.doi.org/10.1080/00207721.2021.1890271.
[7] M.H. Trinh, S. Zhao, Z. Sun, D. Zelazo, B.D.O. Anderson, H.-S. Ahn, Bearing-based formation control of a group of agents with leader-first follower structure, IEEE Trans. Automat. Control 64 (2) (2019) 598–613, http://dx.doi.org/10.1109/TAC.2018.2836022.
[8] P. Zhang, M. de Queiroz, X. Cai, Three-dimensional dynamic formation control of multi-agent systems using rigid graphs, J. Dyn. Syst., Meas., Control 137 (11) (2015) 111006, http://dx.doi.org/10.1115/1.4030973.
[9] S. Singh, A. Jain, Time-varying distance-constrained formation maneuver control with guaranteed prescribed performance for mobile agents, in: Amer. Control Conf., 2022, pp. 5134–5139, http://dx.doi.org/10.23919/ACC53348.2022.9867847.
[10] Z. Yang, C. Chen, S. Zhu, X. Guan, G. Feng, Distributed entrapping control of multiagent systems using bearing measurements, IEEE Trans. Automat. Control 66 (12) (2021) 5696–5710, http://dx.doi.org/10.1109/TAC.2020.3046714.
[11] H.G. de Marina, Distributed formation maneuver control by manipulating the complex Laplacian, Automatica 132 (2021) 109813, http://dx.doi.org/10.1016/j.automatica.2021.109813.
[12] Z. Han, L. Wang, Z. Lin, R. Zheng, Formation control with size scaling via a complex Laplacian-based approach, IEEE Trans. Cybern. 46 (10) (2016) 2348–2359, http://dx.doi.org/10.1109/TCYB.2015.2477107.
[13] X. Fang, X. Li, L. Xie, Distributed formation maneuver control of multiagent systems over directed graphs, IEEE Trans. Cybern. 52 (8) (2022) 8201–8212, http://dx.doi.org/10.1109/TCYB.2020.3044581.
[14] Y. Xu, D. Luo, H. Duan, Distributed planar formation maneuvering of leader-follower networked systems via a barycentric coordinate-based approach, Sci. China Technol. Sci. 64 (8) (2021) 1705–1718, http://dx.doi.org/10.1007/s11431-020-1797-5.
[15] X. Li, L. Xie, Dynamic formation control over directed networks using graphical Laplacian approach, IEEE Trans. Automat. Control 63 (11) (2018) 3761–3774, http://dx.doi.org/10.1109/TAC.2018.2798808.
[16] S. Zhao, D. Zelazo, Translational and scaling formation maneuver control via a bearing-based approach, IEEE Trans. Control Netw. Syst. 4 (3) (2017) 429–438, http://dx.doi.org/10.1109/TCNS.2015.2507547.
[17] S. Zhao, Affine formation maneuver control of multiagent systems, IEEE Trans. Automat. Control 63 (12) (2018) 4140–4155, http://dx.doi.org/10.1109/TAC.2018.2798805.
[18] Y. Xu, S. Zhao, D. Luo, Y. You, Affine formation maneuver control of high-order multi-agent systems over directed networks, Automatica 118 (2020) 109004, http://dx.doi.org/10.1016/j.automatica.2020.109004.
[19] Y. Xu, D. Luo, Y. You, Affine transformation based formation maneuvering for discrete-time directed networked systems, Sci. China Technol. Sci. 63 (2020) 73–85, http://dx.doi.org/10.1007/s11431-018-9456-0.
[20] Y. Tang, D. Zhang, P. Shi, W. Zhang, F. Qian, Event-based formation control for nonlinear multiagent systems under DoS attacks, IEEE Trans. Automat. Control 66 (1) (2021) 452–459, http://dx.doi.org/10.1109/TAC.2020.2979936.
[21] B. Cheng, Z. Wu, Z. Li, Distributed edge-based event-triggered formation control, IEEE Trans. Cybern. 51 (3) (2021) 1241–1252, http://dx.doi.org/10.1109/TCYB.2019.2910131.
[22] J. Liu, J.-a. Fang, Z. Li, G. He, Formation control with multiple leaders via event-triggering transmission strategy, Internat. J. Systems Sci. 17 (6) (2019) 1494–1506, http://dx.doi.org/10.1007/s12555-018-0320-6.
[23] J. Wang, X. Ma, H. Li, B. Tian, Self-triggered sliding mode control for distributed formation of multiple quadrotors, J. Franklin Inst. 357 (17) (2020) 12223–12240, http://dx.doi.org/10.1016/j.jfranklin.2020.09.008.
[24] W. Li, H. Zhang, W. Wang, Z. Cao, Fully distributed event-triggered time-varying formation control of multi-agent systems subject to mode-switching denial-of-service attacks, Appl. Math. Comput. 414 (2022) 126645, http://dx.doi.org/10.1016/j.amc.2021.126645.
[25] Z. Yan, L. Han, X. Li, X. Dong, Q. Li, Z. Ren, Event-Triggered formation control for time-delayed discrete-Time multi-Agent system applied to multi-UAV formation flying, J. Franklin Inst. 360 (5) (2023) 3677–3699, http://dx.doi.org/10.1016/j.jfranklin.2023.01.036.
[26] X. Chai, J. Liu, Y. Yu, C. Sun, Observer-based self-triggered control for time-varying formation of multi-agent systems, Sci. China Inf. Sci. 64 (3) (2021) 132205, http://dx.doi.org/10.1007/s11432-019-2815-7.
[27] M. Ranjbar, M.T.H. Beheshti, S. Bolouki, Event-based formation control of networked multi-agent systems using complex Laplacian under directed topology, IEEE Control Syst. Lett. 5 (3) (2021) 1085–1090, http://dx.doi.org/10.1109/LCSYS.2020.3009747.
[28] W. Zhu, W. Cao, Z.-P. Jiang, Distributed event-triggered formation control of multiagent systems via complex-valued Laplacian, IEEE Trans. Cybern. 51 (4) (2021) 2178–2187, http://dx.doi.org/10.1109/TCYB.2019.2908190.
[29] W. Zhu, W. Cao, M. Yan, Q. Li, Event-triggered formation control of multiagent systems with linear continuous-time dynamic models, IEEE Trans. Syst., Man, Cybern., Syst. 52 (10) (2022) 6235–6245, http://dx.doi.org/10.1109/TSMC.2022.3144161.
[30] J. Wang, J. Gao, P. Wu, Attack-resilient event-triggered formation control of multi-agent systems under periodic DoS attacks using complex Laplacian, ISA Trans. 128 (2022) 10–16, http://dx.doi.org/10.1016/j.isatra.2021.10.030.
[31] Z. Chang, J. Wang, Z. Li, Fully distributed event-triggered affine formation maneuver control over directed graphs, IFAC-PapersOnLine 55 (3) (2022) 178–183, http://dx.doi.org/10.1016/j.ifacol.2022.05.031.
[32] J. Yang, H. Yu, T. Chen, Affine formation maneuver control of event-triggered multi-agent systems, IFAC-PapersOnLine 53 (2) (2020) 3391–3396, http://dx.doi.org/10.1016/j.ifacol.2020.12.2540.
[33] Z. Lin, L. Wang, Z. Chen, M. Fu, Z. Han, Necessary and sufficient graphical conditions for affine formation control, IEEE Trans. Automat. Control 61 (10) (2016) 2877–2891, http://dx.doi.org/10.1109/TAC.2015.2504265.
[34] E. Frank, On the zeros of polynomials with complex coefficients, Bull. Amer. Math. Soc. 52 (2) (1946) 144–157, http://dx.doi.org/10.1090/S0002-9904-1946-08526-2.
[35] W. Zhu, Z.-P. Jiang, Event-based leader-following consensus of multi-agent systems with input time delay, IEEE Trans. Automat. Control 60 (5) (2015) 1362–1367, http://dx.doi.org/10.1109/TAC.2014.2357131.
[36] W. Zhu, H. Pu, D. Wang, H. Li, Event-based consensus of second-order multi-agent systems with discrete time, Automatica 79 (2017) 78–83, http://dx.doi.org/10.1016/j.automatica.2017.01.042.
[37] K. Zhang, B. Gharesifard, E. Braverman, Event-triggered control for nonlinear time-delay systems, IEEE Trans. Automat. Control 67 (2) (2022) 1031–1037, http://dx.doi.org/10.1109/TAC.2021.3062577.
[38] Y. Zhao, C. Xian, G. Wen, P. Huang, W. Ren, Design of distributed event-triggered average tracking algorithms for homogeneous and heterogeneous multiagent systems, IEEE Trans. Automat. Control 67 (3) (2022) 1269–1284, http://dx.doi.org/10.1109/TAC.2021.3060714.
[39] C. Xian, Y. Zhao, Z.-G. Wu, G. Wen, J.-A. Pan, Event-triggered distributed average tracking control for Lipschitz-type nonlinear multiagent systems, IEEE Trans. Cybern. 53 (2) (2023) 779–792, http://dx.doi.org/10.1109/TCYB.2022.3159250.

[40] G. Miao, J. Cao, A. Alsaedi, F.E. Alsaadi, Event-triggered containment control for multi-agent systems with constant time delays, J. Franklin Inst. 354 (15) (2017) 6956–6977, http://dx.doi.org/10.1016/j.jfranklin.2017.08.010.

[41] W. Zou, Z. Xiang, Event-triggered containment control of second-order nonlinear multi-agent systems, J. Franklin Inst. 356 (17) (2019) 10421–10438, http://dx.doi.org/10.1016/j.jfranklin.2018.05.060.

[42] T. Li, Z. Li, S. Fei, Z. Ding, Second-order event-triggered adaptive containment control for a class of multi-agent systems, ISA Trans. 96 (2020) 132–142, http://dx.doi.org/10.1016/j.isatra.2019.06.003.

[43] Y. Zhou, Y. Pan, S. Li, H. Liang, Event-triggered cooperative containment control for a class of uncertain non-identical networks, Appl. Math. Comput. 375 (2020) 125065, http://dx.doi.org/10.1016/j.amc.2020.125065.